

Analysis of Large-Scale Multi-Tenant GPU Clusters for DNN Training Workloads

Myeongjae Jeon^{†*}, Shivaram Venkataraman^{‡*}, Amar Phanishayee^{*},
Junjie Qian^{*}, Wencong Xiao^{§*}, and Fan Yang^{*}

[†]UNIST [‡]University of Wisconsin [§]Beihang University ^{*}Microsoft Research

Abstract

With widespread advances in machine learning, a number of large enterprises are beginning to incorporate machine learning models across a number of products. These models are typically trained on shared, multi-tenant GPU clusters. Similar to existing cluster computing workloads, scheduling frameworks aim to provide features like high efficiency, resource isolation, fair sharing across users, etc. However Deep Neural Network (DNN) based workloads, predominantly trained on GPUs, differ in two significant ways from traditional big data analytics workloads. First, from a cluster utilization perspective, GPUs represent a monolithic resource that cannot be shared at a fine granularity across users. Second, from a workload perspective, deep learning frameworks require gang scheduling reducing the flexibility of scheduling and making the jobs themselves inelastic to failures at runtime. In this paper we present a detailed workload characterization of a two-month long trace from a multi-tenant GPU cluster in Microsoft. By correlating scheduler logs with logs from individual jobs, we study three distinct issues that affect cluster utilization for DNN training workloads on multi-tenant clusters: (1) the effect of gang scheduling and locality constraints on queuing, (2) the effect of locality on GPU utilization, and (3) failures during training. Based on our experience running a large-scale operation, we provide design guidelines pertaining to next-generation cluster schedulers for DNN training workloads.

1 Introduction

Recent advances in machine learning have led to tremendous improvements in tasks ranging from object detection [30] to speech recognition [33] and language translation [47]. As a result a number of enterprises are now incorporating machine learning models in various products [1, 4]. To facilitate model training, enterprises typically setup a large cluster shared by users belonging to a number of different production groups. Similar to clusters setup for big data analysis [12, 50], using

shared clusters can facilitate better utilization and reduce development overheads.

However deep learning workloads pose a number of new requirements or constraints on cluster management systems. Since machine learning algorithms are floating point computation intensive, these workloads require hardware accelerators like GPUs. However, unlike CPUs, accelerators do not typically have proper hardware support for fine-grained sharing [21]. While there are software mechanisms to enable sharing, they often have high overhead making it challenging to share resources across jobs [40, 53]. Furthermore, training on large datasets often requires the use of multiple GPUs [20] and machine learning frameworks typically require that tasks on each GPU be scheduled at the same time, i.e., gang scheduled [18]. This increases the risk of resource fragmentation and low utilization in shared clusters. Finally, multi-GPU training also implies synchronization of model parameters across GPUs and hence it is important to achieve better *locality* while scheduling to allow for the use of faster interconnects for both intra- and inter-machine communication.

Despite their growing popularity, to the best of our knowledge, there has been no systematic study of multi-tenant clusters used to train machine learning models. In this paper, we present the design of a large, multi-tenant GPU-based cluster used for training deep learning models in production. We describe Philly, a service in Microsoft for training machine learning models that performs resource scheduling and cluster management for jobs running on the cluster. Using data from this system, we then present a detailed workload characterization and study how factors such as gang scheduling, locality requirements and failures affect *cluster utilization*.

Our analysis spans across two months and uses around 100,000 jobs run by hundreds of users. We combine logs from Apache YARN [48], our cluster scheduler, utilization information from Ganglia [32], and logs from each job to perform a systematic analysis of cluster utilization.

We study two main aspects of how locality-aware scheduling affects performance and utilization. First, we study how waiting for locality constraints can influence queuing delays

before training jobs are run. Training jobs need to be gang scheduled, as hyper-parameters are picked for specific GPU count configurations. Given that training jobs take a long time to run, and greater locality improves performance due to the availability of faster interconnects for parallel training [52], the scheduler in Philly waits for appropriate availability of GPUs before beginning to run the training job. Our study shows that as one might expect, relaxing locality constraints reduces queueing delays, especially for jobs that use many GPUs – our emphasis here is not on presenting this as a new insight, but instead on highlighting this using real-world data from production clusters.

Next, we study how locality-aware scheduling can affect the GPU utilization for distributed training jobs. Even though most GPUs within a cluster are allocated to users, thus *suggesting* high cluster utilization, this metric alone is misleading. We show that the hardware utilization of GPUs in use is only around 52% on average. We investigate two reasons which contribute to low GPU utilization: (1) the *distribution* of *individual* jobs across servers, ignoring locality constraints, increases synchronization overheads, and (2) the *colocation* or packing of *different* jobs on same server leads to interference due to contention for shared resources.

Finally, we look at why jobs might fail to complete successfully and offer a detailed characterization of the causes for such failures in our clusters. Around 30% of jobs are killed or finish unsuccessfully due to failures. Failures are caused by errors across the stack, with programming errors dominating failures and occurring early in the training process; failures due to cluster components like HDFS tend to occur much later in the training lifecycle.

Based on the lessons learnt from data analysis and our experiences running a large-scale operation over the years, we provide three guidelines to improve the next generation of cluster schedulers for DNN workloads. First, because the lack of locality impacts both utilization and job runtime, and because DNN training jobs are long running, schedulers should trade queueing delay for adhering to locality constraints. Second, different jobs that share a single server may interfere with each other and thus adversely affect their training time. Schedulers should thus aim to isolate the jobs on dedicated servers while implementing techniques like migration for defragmentation, to support the locality constraints of jobs that need more GPUs. Third, many failures ought to be caught early, well before they are scheduled on a larger shared cluster. This can be achieved by scheduling each incoming job on a small dedicated pool of servers or even using a single GPU should be able to catch simple programming and configuration errors from multi-GPU jobs. Furthermore, an online analysis of failures at runtime can let schedulers adapt their retry policies thus avoiding wasteful re-execution.

Philly’s design does not stand in isolation. There are many open platforms for DNN job scheduling that use designs similar to Philly, e.g., OpenPAI [35] and Submarine [44]. We

hope that insights and data from our study, and the accompanying traces [38], inform the burgeoning work of scheduling research for machine learning workloads.

2 Philly: System Overview

In this section we provide an overview of the design and architecture of Philly. First, we describe the workloads that are supported in our system and then describe the hardware characteristics of the clusters. Next, we describe the lifecycle of a job. Finally, we explain our data collection pipeline and highlight the data we use to perform our analysis in subsequent sections. The authors would like to note that Philly has been developed over the past few years by a team of developers in our company and has gone through multiple generations of design.

2.1 Workloads

Philly is designed to support workloads that perform supervised machine learning where jobs learn a model given training data and the corresponding labels. This includes training jobs from production groups developing products that use models for image classification, speech recognition, etc. The system supports jobs written using any machine learning framework like TensorFlow [5], CNTK [42], Caffe [28], and PyTorch [39]. Jobs are based on recently proposed learning architectures like convolutional neural networks [30], LSTMs [45] and RNNs [34].

All jobs, irrespective of the framework or model being used, rely on iterative optimization methods [19] like stochastic gradient descent (SGD). In each iteration, the gradient computation is performed by translating the model components into code that can be executed on accelerators like GPUs. The gradient values are then aggregated to compute a model update and these iterations are repeated until convergence. Training a model could require thousands to millions of iterations [46], and result in multiple passes or *epochs* over the entire dataset.

To scale training across larger datasets, a number of jobs use distributed training across machines. Distributed training typically uses data parallelism where each worker loads a complete copy of the model into its own memory. In each iteration, every worker performs training using a subset of the input data, and at the end of the iteration all workers exchange gradients to synchronize model updates. This synchronization phase is performed using either parameter servers [31] or high performance libraries for collective communication (such as MPI, NCCL, etc).

2.2 Cluster Architecture

Our system is deployed on large GPU clusters shared across many groups in the company. Our clusters has grown significantly over time, both in terms of the number of machines

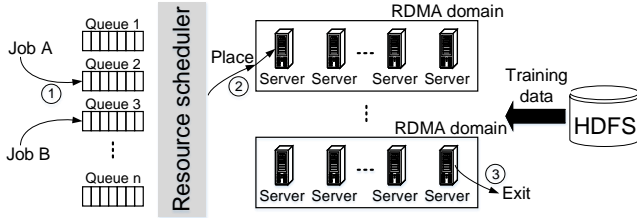


Figure 1: The lifecycle of deep learning jobs in Philly.

(5× increase in one year) as well as the number of GPUs per machine (2-GPU to 8-GPU servers).

Our clusters have high-speed network connectivity among servers and GPUs in the cluster. This is to speed up distributed training where workers need to exchange model updates promptly for every iteration. There is a hierarchy of network links available in our cluster for communication across GPUs. For example, machines within the same rack (*RDMA domain*) are connected via 100-Gbps RDMA (InfiniBand) network, while cross-rack traffic goes through Ethernet. To improve communication performance, workers in a distributed training job must either be colocated on the same machine or preferably communicate over a higher-speed network such as say InfiniBand. Thus, our framework considers both GPUs and network connectivity for scheduling.

Similar to existing big data analytics clusters, our clusters use HDFS [43] as the distributed storage system and our resource manager is based off Apache YARN [48]. Input data for the machine learning jobs is stored in HDFS and read by jobs during training. Users provide a Docker container with their training code and its dependencies. Each training job requests 1 or more GPUs which can be allocated across multiple machines. Philly instantiates one container per machine allocated to the job when it is scheduled for execution.

2.3 Job Scheduling and Execution Workflow

Figure 1 shows the lifecycle of a deep learning job in Philly and the various stages of execution that it goes through.

Incoming jobs and queueing ①. As a part of job submission, users specify *the number of GPUs* required. To facilitate host resource allocation, we perform an allocation of CPU cores and memory capacity proportional to the requested GPU count. Once a job has been received by the scheduler it is queued while the necessary GPUs are allocated. To support multiple production groups we create a virtual cluster for each group and associate a *resource share* or *quota* in terms of number of GPUs to each virtual cluster. Each virtual cluster has a separate allocation queue in Apache YARN and we use the Fair Scheduler to manage these queues [2]. Our scheduler not only respects the configured resource shares but also allocates unused GPUs to a queue which has additional demand. Jobs can be preempted based on fair share of resources among

virtual clusters. Our scheduler starts preemption only when a majority (90%) of total GPUs are being used.

For distributed learning, deep learning frameworks require all the GPUs to be available at the same time [21]. Thus the scheduler needs to perform *gang scheduling* while being *locality-aware*, i.e., pack a job’s GPUs onto the smallest number of servers and within an RDMA domain. Locality awareness improves training time by bringing down the time needed for parameter synchronization [21, 52] due to the availability of: (i) fast intra-server interconnects (such as PCIe and NVLink), and (ii) for jobs that do not fit on a single server, high-bandwidth links available within an RDMA domain. We implement these goals by acquiring resources for a job as GPUs become available and waiting for a pre-specified timeout (2–3 minutes in our setup) to acquire all the necessary GPUs with the locality constraints. To facilitate locality-aware GPU scheduling, our job scheduler keeps track of all idle GPUs in the cluster and ranks the corresponding racks and servers. Specifically, racks are ranked by increasing order of allocation or occupancy, and the machines in a rack are ordered the same way. This allows the scheduler to first consider racks and then servers within those racks that have most GPUs available.

If the request is not fulfilled by the timeout, any partially acquired resources are relinquished and we retry scheduling after a back-off (2 minutes in our setup). To avoid starvation, the locality constraints are relaxed after a scheduling request has been retried a fixed number of times. We analyze corresponding queuing delays in Section 3.1.

Job placement and utilization ②. While the scheduler tries to maximize locality for distributed jobs as described before, at the same time the scheduler also aims to avoid fragmentation of resources from smaller jobs (e.g., 1-GPU jobs) by packing them into a fewer servers. However colocating different jobs on the same server could lead to lower GPU utilization due to interference in shared system resources such as PCIe bus [52]. In order to better understand this trade-off we study the effects of colocation vs. distribution and measure how that affects utilization.

Once the job is scheduled to run, its GPUs are *not shared* with other jobs. This is because model training can be computation intensive and we need consistent performance among workers of the job without having stragglers. However, dedicated GPUs may be underutilized for many reasons, e.g., inefficiencies in the code generated by the machine learning frameworks or programs blocking on I/O when reading data from storage. GPU underutilization also comes from distributed training where computation may block during model synchronization among the workers. We analyze the effects of job placement and GPU utilization in Section 3.2.

Table 1 qualitatively compares Philly with the state-of-the-art DNN cluster schedulers, showing both similarities and differences exist. Nonetheless, locality and colocation are the common issue for all contemporary clusters, and that insights

Table 1: Comparison of DNN cluster schedulers. JCT means job completion time.

	Philly	Gandiva [52]	Optimus [37]	Tiresias [21]
Objective	Consolidation	Consolidation	Average JCT	Average JCT
Algorithm	Locality-based	Time-sharing	SRTF	Gittins Index & LAS
Input	Arrival time	N/A	Remaining time	Attained service
Preemption	Model checkpoint	Context switch	Model checkpoint	Model checkpoint

obtained in this study are widely valuable.

Training progress and completion ③. Jobs can finish with one of three statuses: passed, killed, or unsuccessful. Passed indicates that the job completed successfully, while killed indicates that the job was terminated by the user.

Among successful jobs, every job runs a number of iterations to improve the model incrementally, and the number of iterations to run is typically a static parameter set by the user. In cases where a job is configured with too many iterations, it is possible to deliver the same (or similar) quality of trained model with fewer iterations. Failed jobs in our system are retried a fixed number of times. This is useful for overcoming non-deterministic failures and if the job does not succeed after retries then it is marked as unsuccessful. As failures also contribute to ineffective cluster utilization, we perform a detailed study to understand the reasons behind failures in Section 4.2.

While our focus in this section is specifically about the lifecycle and execution flow in Philly, there are many open platforms for ML job scheduling that use a similar design. Platforms like OpenPAI [35] and Submarine [44] also use a centralized scheduler with support for running machine learning frameworks as Docker containers. While the details of the scheduling algorithm vary across systems, a number of aspects we study in this paper are independent of the choice of scheduler: e.g., failures due to programming errors and bugs in popular frameworks, effect of distributed training across machines, etc. Thus, we believe that lessons from Philly are generally applicable to other clusters as well.

2.4 Data Collection and Analysis

The cluster under study consists of hundreds of machines accounting for thousands of GPUs of the same model. The cluster has 2 server SKUs – one with 2 GPUs per server and another with 8 GPUs per server; RDMA domains are homogeneous with respect to server SKUs. To get a comprehensive understanding of the characteristics of our system and workloads, we developed a data collection and analysis pipeline and collect logs over a 75-day period from Oct. 2017 to Dec. 2017. Our logs contain a total of 96260 jobs over 14 virtual clusters.

The analysis pipeline combines three main log sources in our system as follows. (1) We collect the YARN scheduler logs to obtain job arrival time, number of GPUs requested, GPU allocation status, and job finish status. (2) We collect stdout and stderr logs from the machine learning frameworks

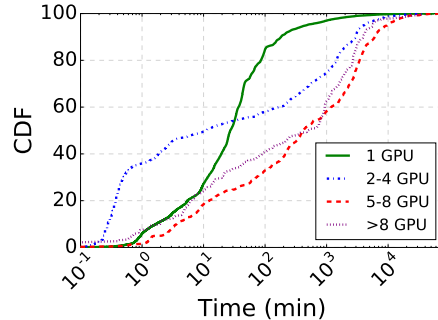


Figure 2: CDF of job run times for 1 GPU, 2-4 GPU, 5-8 GPU, and >8 GPU jobs.

that execute scheduled jobs. (3) We collect logs from Ganglia monitoring system that reports per-minute statistics on hardware usage on every server, including CPU, memory, network, and GPU utilizations. Combined with GPU allocation status in YARN scheduler logs, we can track how a scheduled job utilizes cluster hardware resources.

Our collected data contains jobs from a wide spectrum in terms of their run times and sizes, and consequently cluster resources demands. Jobs run from minutes to days or even weeks, as shown in Figure 2. In contrast, in big data analytics, job execution times range from only tens of milliseconds to a few hours [11, 36, 41]. Furthermore, we see that our workload has significant skewness in run time, with around 0.5% jobs taking more than a week to be finished. Figure 2 also shows how jobs of different sizes vary in terms of execution times. We see that jobs with more GPUs tend to run longer. This results in most of the cluster resources demands coming from the larger jobs, and resource availability status changing relatively slowly over time.

3 Impact of Locality Awareness

Our scheduler trades off locality for lower waiting. Thus placement choices made by the scheduler affect the efficiency of DNN training in two parts: queueing delay (before job execution) and hardware utilization of in-use GPUs (after job execution). The effect of locality constraints on queueing delays has been extensively explored in large-scale resource allocation [7, 11, 25, 54]. Machine learning workloads introduce similar constraints driven by gang scheduling and the requirement for using fast interconnects. In Section 3.1, we an-

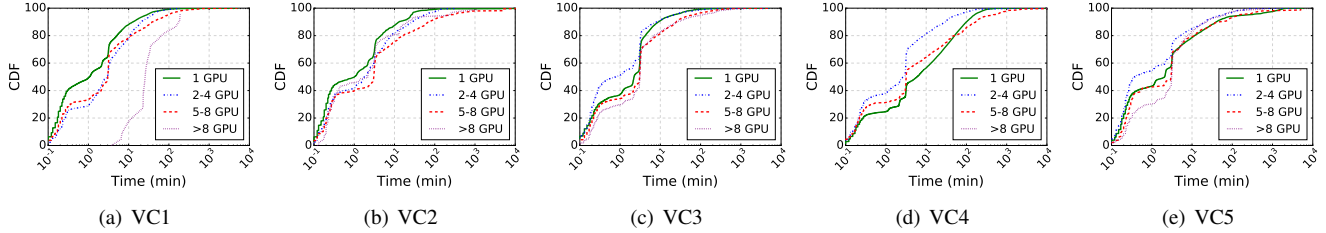


Figure 3: CDF of scheduler queueing delay for five of the largest virtual clusters in our deployment. Note that VC4 contains no jobs with >8 GPU.

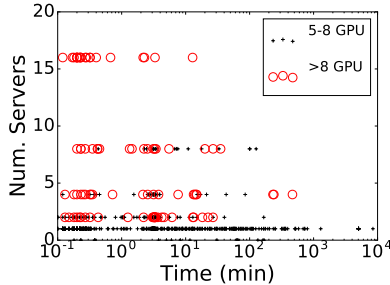


Figure 4: For a given GPU count, relaxing locality constraints reduces queueing delays (VC2).

analyze queueing delays in the context of DNN training cluster using real-world data in detail. Next, we study utilization of processing cycles for GPUs allocated to training jobs in Section 3.2. In particular, while prior work discusses efficiency of distributed training for a certain job size or a configured placement [21, 52], we perform an analysis on the aggregated efficiency for a range of job sizes for the first time.

3.1 Queueing Delays

We first consider overall queueing delay observed during job scheduling. We plot the CDF of queueing delay in Figure 3 for all jobs in five of the largest virtual clusters (VCs). Jobs that need more than 4 GPUs tend to have a slightly longer tail in the distribution of queueing delays compared to their 1 GPU and 2-4 GPU counterparts. For example for VC2, 25% of jobs using >4 GPUs, which include both 5-8 GPU and >8 GPU, experience a queueing delay of at least 10 minutes; in comparison, only 10% of 1 GPU jobs experience a queueing delay of at least 10 minutes.

But overall, queueing delays for jobs, irrespective of their GPU demand, are not markedly distinct. This is partially a consequence of our scheduling policy that chooses to relax locality constraints in order to start a job without incurring a very long queueing delay penalty. To highlight the relation between locality constraints and queueing delays, we next consider jobs with 5-8 GPU and >8 GPU. We correlate scheduler waiting times with number of servers on which the

Delay	2-4 GPU	5-8 GPU	>8 GPU
Fair-share	5168 (40.6%)	3793 (25.8%)	66 (2.1%)
Fragmentation	7567 (59.4%)	10928 (74.2%)	3117 (97.9%)

Table 2: Frequencies of two types of queueing delay.

jobs are placed, and show the results in Figure 4. As expected, most of jobs with 5-8 GPU are scheduled with high locality, i.e., placed on one or two servers. On the other hand, we find that jobs with >8 GPU are spread across a wider range from 2 to 16 servers. Clearly, when jobs end up running on 16 servers, they start execution much sooner than running on 2 or 4 servers. This confirms how our scheduler works in practice to trade-off locality for lower scheduling delay.

While effective, we find that this decision affects the GPU utilization as discussed in Section 3.2. We next look at more details on the queueing delay characteristics and break down the delay by different causes.

3.1.1 Impact of Locality-Driven Scheduling

Queueing delay can be caused by two primary factors: fairness (which is common in conventional data analytics clusters), and locality requirement and resource fragmentation (which is more prevalent in deep learning clusters). We call queueing caused by the first factor as *fair-share delay*, as it happens when the virtual cluster uses up its assigned quota (i.e., number of GPUs). However, it is possible that a job arrives within the quota but fails to be scheduled, mainly because resource fragmentation makes it hard to find enough GPUs with high locality. We call this queueing delay as *fragmentation delay*. In practice, we find that resource fragmentation is very common. For example, we observe that (i) when two thirds of the total GPUs are being used, the fraction of servers that are completely empty is less than 4.5% and that (ii) these servers are spread across RDMA domains.

We next see how frequently fair-share delay and fragmentation delay occur for different job sizes in our workloads. Since some jobs are quickly terminated, we only consider jobs that run for at least one minute. Further, since fragmentation influences distributed training jobs only, we consider jobs that

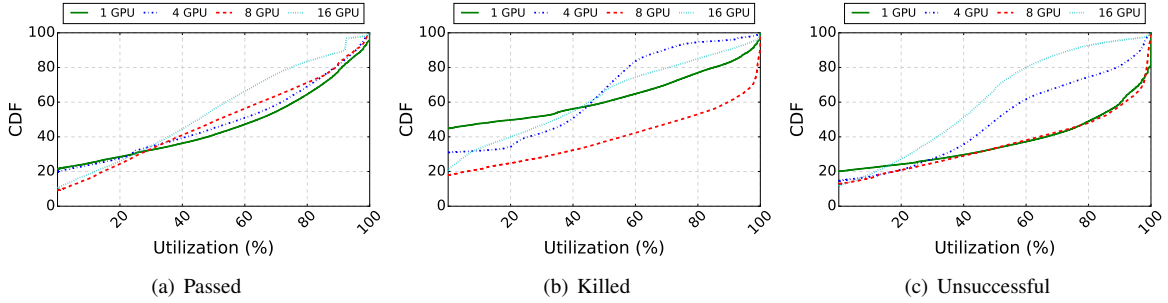


Figure 5: CDF of per-minute GPU utilization for passed, killed, unsuccessful jobs in different sizes.

use 2 or more GPUs. Table 2 shows the frequencies for the two types of delay. For jobs with 5-8 GPU, fragmentation delay is responsible for 74.2% of occurrences, and it dominates for larger jobs. In contrast, for smaller jobs, we see that the two causes are more balanced. Further, we also observe that across all jobs fragmentation delay is responsible for around 80% of the delay in terms of waiting time. This is because fair-share delays are easy to mitigate with preemption, but fragmentation delays are much harder to overcome in our current design.

Finally, we note that the queuing delay fractions vary across virtual clusters. Among the five largest virtual clusters, VC5 often over-subscribes its quota and thus the proportion of fair-share delay is overall higher at 37%.

Does out-of-order scheduling exacerbate job queuing?

Given the resource fragmentation and the fact that the YARN scheduler is work-conserving, larger jobs could be additionally negatively affected by out-of-order scheduling. To see how, consider a job that requires 24 GPUs spread across three machines. While this job is waiting for such configuration, if a smaller job requests 2 GPUs, it is scheduled on machines where two GPUs become available. This could cause further fragmentation and lead to the 24-GPU job needing to retry after a backoff. In our workload, out-of-order scheduling is quite common, with 38.1% of scheduling decisions, and occurs 100% for jobs with 5-8 GPU or >8 GPU. However, we find that most out-of-order scheduling decisions do not greatly affect the waiting time for resource-intensive jobs. For example, for out-of-order scheduling occurrences of jobs with 5-8 GPU or >8 GPU, as much as 85.0% corresponds to cases where idle GPUs are effectively utilized without prolonging the scheduling time of those waiting jobs.

In summary, our analysis shows why it makes sense to relax locality over time to mitigate queuing delays for distributed training. We also find that in addition to fair-share queuing delay, the need for gang scheduling and locality introduces fragmentation delay for machine learning jobs.

Job size	Passed	Killed	Unsuccessful	All
1 GPU	53.51	37.02	62.82	52.38
4 GPU	51.13	34.39	50.95	45.18
8 GPU	51.09	60.63	64.34	58.99
16 GPU	44.88	36.98	39.02	40.39
All	52.43	42.98	60.43	52.32

Table 3: Mean GPU utilization for different job sizes.

3.2 GPU utilization

GPUs are the most expensive resources in our cluster and this makes their efficiency an important factor in assessing the cost-effectiveness across the entire cluster. For each individual GPU, Ganglia [32] reports aggregate performance counters every minute, including utilization of processing cycles and memory, temperature, power usage, etc [3]. We next present how efficiently training jobs use processing cycles in their (exclusively) allocated GPUs. Note that our current generation of GPUs only report coarse-grained utilization for processing cycles that can only be used to detect if any of the streaming multiprocessors (SMs) are being utilized [3]. They do not report what fraction of the SMs are being actually used within a single GPU. Therefore, our analysis presents an “upper bound” of actual effective SM utilization.

Overall, deep learning training jobs underutilize GPU processing cycles regardless of their job sizes. Figure 5 shows CDFs of per-minute GPU utilization of passed, killed, and unsuccessful jobs for different sizes. Table 3 reports averages for each job size, including averages for different job status; we use these job sizes as representative of small, medium and large jobs based on the GPU request distribution in our cluster. Surprisingly we find that around 47.7% of in-use GPUs’ cycles are wasted across all jobs, with jobs using 16 GPUs exhibiting the lowest utilization at 40.39%. Moreover, across job status in Figure 5, the median utilization for 16 GPU jobs is 45.00%, 34.24%, 39.54% for Passed, Killed, and Unsuccessful, respectively. These are 6.46%, 40.25%, and 42.63% lower than the 8 GPU jobs in the corresponding job status. We study the efficiency of such jobs in the next section in detail.

Metric	SameServer	DiffServer	IntraServer	InterServer
GPU util.	57.7	49.6	37.5	36.5
Images/s	114.8	98.0	75.6	74.1

Table 4: Mean GPU utilization and training performance of ResNet-50 over different locality/colocation configurations.

3.2.1 Impact of Distributed Learning

Given that the 8 GPUs mounted in each server can communicate more efficiently without using the network, our job scheduling strategy is to favor intra-server locality when assigning each job to available GPUs. At the same time, the scheduler attempts to pack small jobs into fewer servers to avoid fragmentation. This leads to *job colocation* on the same server and consequently could lead to interference in shared system resources (e.g., RDMA and PCIe) [52]. This creates an interesting utilization spectrum for multi-GPU jobs. In particular, jobs using more than 8 GPUs must *distribute* training instances across multiple servers and may be dynamically colocated with other jobs. This scenario also involves communication overheads since each server has to periodically wait for model aggregation to happen over the network.

To confirm that such distribution and colocation factors indeed relate to the efficiency of GPUs in use, we first characterize utilization of processing cycles for various job placement scenarios using a popular image recognition model, ResNet-50 [22]. Specifically we train ResNet-50 with 2 GPUs using TensorFlow and perform offline experiments with placements that exercise shared resources differently. Then using our telemetry data, we attempt to infer correlations between those factors and the observed efficiency in our cluster.

Analysis using ResNet-50. Table 4 shows the impact of distribution only, by comparing a ResNet-50 job placed in a single server (SameServer) with the job placed in two servers connected with RDMA network (DiffServer). Each server has four NVIDIA Tesla P100 GPUs attached to a CPU socket. The table reports GPU utilization when processing a batch size of 32 images during training. First we observe that the training does not fully utilize GPUs even for single machine execution. In particular, SameServer achieves utilization of 57.7% for GPUs in use. It increases to 71.1% for twice the batch size but only increases marginally for larger batches. Also the table shows that using distributed training achieves lower utilization of 49.6% in DiffServer. This shows that even for 2-GPU jobs, there is a cost to not achieving locality.

Given a distributed training setup, contention for shared resources like RDMA and PCIe further lowers the efficiency of utilized GPUs. To show this we set DiffServer as our baseline and measure changes in the efficiency while populating additional ResNet-50 jobs in the same servers. First, we measure GPU utilization when the colocated jobs do not use RDMA network at all: we place two SameServer jobs, one on each server in the same CPU socket as the job under

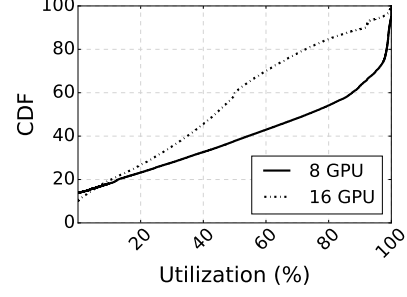


Figure 6: GPU utilization when running 8 and 16 GPU jobs on dedicated servers.

study. Thus, these jobs interfere with the job under study in the use of PCIe buses while reading training inputs, aggregating model updates, and so on. The observed efficiency is shown as IntraServer in Table 4, and we see that having such intra-server interference lowers the utilization by as much as 12.1%. We also study if such interference matters for the RDMA network in InterServer. For this setup we use two DiffServer jobs instead of two SameServer jobs as background traffic, so that all the jobs are distributed across two servers and share the RDMA network. In this case, we see a 13.1% decrease in utilization compared to the baseline.

Our experimental study reveals that efficiency of allocated GPUs varies according to locality and colocation scenarios that could occur in the cluster. Further, any placement that causes lowered GPU utilization also results in slowdown in training performance (i.e., images processed per second) as shown in Table 4. Next, we analyze utilization for our aggregate workload. We note that unlike the controlled experiment, the type of model trained and the batch sizes used vary across jobs in our aggregate workload making it harder to establish a baseline utilization without distribution or inference.

Distributed training with dedicated servers. First, to study the effects of distribution, we restrict our study to look at 8 GPU and 16 GPU jobs that are packed on one or two servers. In this case, the 8 GPU jobs uses all 8 GPUs in a single server while the 16 GPU jobs uses all the GPUs in two servers. The network over which the servers for these jobs are connected to each other is shared. Figure 6 shows the results of our comparison. Compared to the 8 GPU jobs, we see that 16 GPU jobs, which have the additional model aggregation step in distributed mode, have significantly lower utilization. Specifically, for 8 GPU jobs, GPU cycles are utilized 56.9% of time on average while this is only 34.3% for 16 GPU jobs. Furthermore, the median is 73.12% for 8 GPU jobs, which is 1.67x the median in the 16 GPU case.

Distributed training with shared servers. When locality constraints are relaxed, a job may have to be distributed over many servers while sharing them with other jobs. Distributing a job over many shared servers can further lower utilization of GPUs. This drop in utilization occurs not only due to a higher network overhead but also because of interference from

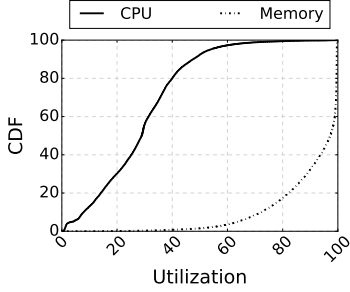


Figure 7: Host resource utilization.

Degree	Mean	50%ile	90%ile	95%ile
2 servers	43.66	43.69	91.77	97.06
4 servers	40.94	39.85	83.28	91.97
8 servers	28.56	25.71	65.68	78.85

Table 5: GPU utilization for 16-GPU jobs that are spread over 2, 4, and 8 servers.

unrelated but co-located jobs. To study this, we see how the GPU utilization of 16-GPU jobs varies as we move from dedicated GPUs to a larger number of shared servers. Table 5 shows the average and percentiles for GPU utilization across the different allocation scenarios.

When running on 2 8-GPU servers, a 16-GPU job has dedicated servers. When running on 4 servers, the 16-GPU job may occupy 4 GPUs on each server, and will be colocated with other jobs on those servers. We find that the degree of interference is larger if the job is distributed on more servers. Table 5 shows that in addition to the inefficiency caused by distribution (Figure 6) there is additional underutilization caused by colocation. We see that for 16-GPU jobs distributed across 8 servers, the average utilization is as low as 28.26% and more than 90% of jobs have less than 66% utilization.

Among host resources, our scheduler dedicates CPU and memory along with GPU to each job. In deep learning clusters, these host resources are used for many useful tasks including caching training inputs, model aggregation, and periodic model validation and progress report. By default, we allocate CPU and memory capacity proportional to the number of requested GPUs. Figure 7 shows CDFs of utilization of these host resources observed in our servers. In general, many servers underutilize CPU cycles yet highly utilize memory. This indicates that a useful feature in the scheduler would be to observe if a particular job requires disproportionate amount of host memory and isolate memory used by jobs colocated on the same server.

In summary, our data analysis shows how GPUs are underutilized in shared clusters. We presented correlations of how distribution and interference affect utilization and validated this using a controlled experiment to break down the importance of locality and interference. We discuss some implications for scheduler design in Section 5.

Status	Count(%)	GPU times used (%)
Passed	66696 (69.3%)	44.53%
Killed	12996 (13.5%)	37.69%
Unsuccessful	16568 (17.2%)	17.76%
Total	96260 (100.0%)	100.0%

Table 6: Distribution of jobs by their final status.

4 Training Progress and Completion

Jobs in our system finish with one of three statuses: passed, killed or unsuccessful. Similar to iterative online computations [6, 16], our machine learning job utilizes cluster resources to improve the model over time. However as opposed to prior study on big data traces [29], we see a significant fraction of jobs (30.7% as shown in Table 6) are either terminated unsuccessfully or killed by users. They constitute around 55% of the total GPU time used during our trace collection period. Thus it is important to understand the reason behind these failures as fewer unsuccessful jobs would mean that more of the cluster resources can be used for successful jobs.

4.1 Effectiveness of Training Iterations

Most deep learning jobs optimize a non-convex loss function and the optimization algorithms do not necessarily guarantee that the loss always decreases with more training. Thus, similar to [21], users in our system submit model training jobs using a larger number of epochs than necessary to get the optimal model. To analyze the magnitude of this effect we study how the training loss for a job varies across epochs and measure the epoch at which we achieve the best training loss. As this information is not printed in the log by every user/framework, we are only able to obtain convergence information for around 2502 jobs.

First, Figure 8(a) shows the fractions of epochs required to reach the lowest loss across all passed jobs. From the figure we see that around 80% of passed jobs require all the epochs executed to reach the lowest loss. We repeat this study for killed jobs and see a similar pattern as shown in Figure 8(b).

However we also see that a majority of jobs improve the loss marginally using a large fraction of epochs. In particular, Figure 8(a) shows the fraction of epochs required to reach within 0.1% of the lowest loss across all passed jobs. Around 75% of jobs reach within 0.1% of the lowest loss using only 40% of the epochs. Again, a similar pattern is shown for killed jobs in Figure 8(b). While we do not present data from our surveys, this suggests that machine learning practitioners can early terminate jobs to save use of GPU times considerably when the loss change is less than a particular threshold in successive epochs. Essentially, we look into how much resources are used to improve 0.1% of convergence accuracy in terms of the fraction of GPU times for each job. In our workload, this accounts for 62% and 56% on average for passed jobs and killed jobs, respectively.

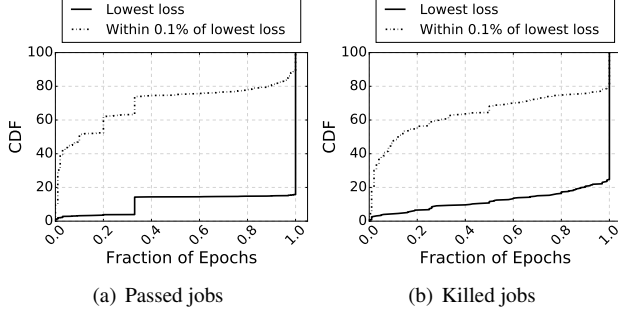


Figure 8: Fraction of epochs necessary to achieve a particular loss threshold for (a) passed jobs and (b) killed jobs.

4.2 Job Failures

We next present a detailed analysis on job failures, including why/when/how frequently jobs fail and what their impact is on effective cluster usage. We remind the reader that in our cluster scheduler, a job is retried upon failure. If the job repeatedly fails it is marked as unsuccessful as further retries are deemed no longer effective. Figure 9 presents a high-level summary of job retries/failures and shows that jobs using more than 4 GPUs not only retry execution more often but also finish unsuccessfully at higher rate. The reasons behind job retries/failures are diverse, and failures occur at different times during job execution. We thus investigate failures by classifying them across layers of our system stack.

4.2.1 Failure Classification

Table 7 presents analysis results of failures based on two classification factors. First, failures are classified from different sources (Column 2): the sources include (i) Infrastructure (IF) which includes YARN, HDFS and all other framework components, (ii) AI Engine (AE) which includes TensorFlow, Torch, and any other platforms, and (iii) User (U) which represents programmers. Column 1 lists a number of reasons for failures we observe from the workload.

Most failure reasons in the table are self-explanatory, and we describe six important ones in more detail here.

- (1) **Incorrect inputs:** Model files or input data stored in the external HDFS storage cannot be read.
- (2) **Semantic error:** Errors that happen due to library version mismatch or other dependencies of the user training program not being setup correctly.
- (3) **Model checkpoint error:** The job is not able to successfully create a model checkpoint after a certain number of epochs complete. This is usually due to either transient error in HDFS or HDFS name node recovery.
- (4) **MPI runtime failure:** This is usually due to either a failure of network connection to peer MPI process, or possibly

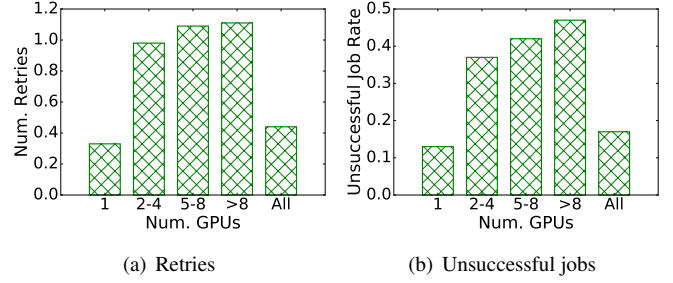


Figure 9: (a) Average number of job retries for using different number of GPUs, and (b) subsequent unsuccessful jobs.

an internal failure of the MPI daemon itself.

(5) **Job preempted:** YARN reclaims any GPU currently in use to schedule another job.

(6) **Invalid memory access:** Training job dies because of violating access on memory address space, e.g., using an invalid pointer value, or having race condition while copying data. This failure is observed in both CPU memory and memory allocated for GPU access.

While bridging failure category and failure reason, we observe that a failure reason can appear in multiple categories, even in all involved categories, as shown in Column 2 of Table 7.

Building failure classifier. There exists causality among various failure reasons. For example, *traceback from crash* is a consequence of an *invalid memory access*. Our first mission in building a classifier is identifying signatures of failure reasons closer to the root cause. We capture root-cause signatures from stdout or stderr logs of a failed job. If not explicit from the logs, we then attempt to capture implicit ones such as *traceback from crash*. In consequence, our classifier has in total **more than 230 rules** to find both explicit signatures and implicit signatures. If there is no signature for a failure, we tag it as *no signature*, which constitutes 4.2% of the total failures.

4.2.2 Failure Frequency

Column 3 of Table 7 summarizes the occurrence frequency of the classified failure reason. *Trial* counts the number of failure events observed in our workload: failure reasons are sorted by it. We further group *Trial* occurrences by job ID (*Job*) and user ID (*User*) to see if failures are localized according to the same job or user.

Failures repeat for the same job/user. Our analysis shows that across failure reasons, failures repeat at both job level and user level. In particular, we measure repetition factors (i.e., *Trial* divided by *Job* or *User*) for top-8 failure reasons, which cover 88.9% of the total failures. The measured repetition factors are 2.3 and 38.8 on average for *Job* and *User*, respectively, meaning a single job and a single user on average cause 2.3 and 38.8 occurrences of failure, respectively, during

Failure Reason	Category			Num Occurrences			RTF: Runtime to Failure (mins)				GPU Demand			RTF×Demand (%)
	IF	AE	U	Trial	Job	User	50%ile	90%ile	95%ile	Total %	1	2-4	>4	
CPU out of memory		✓	✓	12076	2803	65	13.45	17.73	33.97	6.62	11465	235	376	3982320 (8.05)
Incorrect inputs	✓		✓	9690	4936	208	1.87	404.83	2095.73	30.43	5844	2638	1208	11979474 (24.21)
Semantic error	✓		✓	2943	2049	159	2.72	376.00	1436.88	9.22	1603	494	846	8442835 (17.06)
Core dump		✓	✓	2912	1784	122	0.85	72.75	431.65	3.35	1936	496	480	1493632 (3.02)
Invalid mem access			✓	2602	1235	108	1.03	403.50	1357.38	3.82	712	774	1116	2352994 (4.75)
Model ckpt error	✓			1995	948	85	181.67	3728.93	8196.02	21.73	743	384	868	8080374 (16.33)
CUDA failure		✓		1484	571	70	1.32	19.87	82.17	0.62	133	1153	198	357119 (0.72)
Syntax error	✓		✓	1132	883	110	0.58	5.02	12.00	0.19	780	184	168	130094 (0.26)
Traceback from crash	✓	✓	✓	777	271	44	1.02	894.33	1394.07	2.34	356	277	144	863130 (1.74)
MPI error	✓			634	166	28	1.62	3015.27	5143.98	3.70	456	54	124	613059 (1.24)
GPU out of memory		✓		487	261	35	18.53	353.62	2740.28	1.08	237	70	180	1040249 (2.10)
MPI runtime failure	✓			478	420	96	1389.48	13778.60	18090.88	14.63	240	141	97	7593398 (15.34)
Permission error			✓	299	151	37	1.00	8.15	15.85	0.07	56	202	41	15185 (0.03)
Import error	✓		✓	148	148	41	0.67	4.58	10.73	0.06	108	30	10	10803 (0.02)
Job preempted	✓			147	95	34	559.08	2682.85	5892.23	1.66	25	95	27	2338772 (4.73)
CUDA init failed		✓		141	69	20	1.08	2.18	4.63	0.03	16	66	59	64512 (0.13)
Model diverged			✓	84	30	5	1.48	44.37	76.53	0.01	78	5	1	2562 (0.01)
CUDA ver. mismatch		✓		49	49	19	0.83	1.65	1.67	0.00	1	1	47	421 (0.00)
GPU ECC error		✓		10	10	2	26.82	671.92	2035.02	0.03	1	5	4	23575 (0.05)
Output node error			✓	3	3	1	0.85	0.95	0.95	0.00	3	0	0	2 (0.00)
Cannot load libs		✓		1	1	1	0.12	0.12	0.12	0.00	1	0	0	0.12 (0.00)
No signature				1684	698	94	1.87	28.00	95.17	0.42	1235	294	155	102138.03 (0.21)

Table 7: Failures classified into failure reasons (sorted based on the number of occurrences). There are largely three categories that cause the failures: Infrastructure (IF), AI Engine (AE), and User (U). A failure reason may be observed in multiple categories.

the data collection period. The most critical one is *CPU out of memory*, where we see 185.7 as the *User* repetition factor. Interestingly, profiling shows that a certain engineer issued a number of training jobs, all of which suffer from the same out-of-memory issue, resulting in high concentration of failures. This motivates the need for runtime detection mechanisms that can correlate errors from the same user even though her jobs are independent from job management point of view.

User/programming errors lead to a lot of failures. Failures incurred by user errors, such as configuration/syntax/semantic errors in program and script, are dominant. These failures are very prevalent across our top-8 failure reasons. As explained, *CPU out of memory* is the most frequent with its failures significantly concentrated on a few users. Other frequent failures such as *incorrect inputs* and *semantic error* are more spread out across different users. From our profiling, the primary factor that causes those failures is a lot of independent components involved in a training job. For example, by definition, *incorrect inputs* happens when there is a failure in reading model or input data stored in external HDFS store. This is due to any error along the path of accessing data from user program/script to data stored in the HDFS: the path is not correct, data format is inconsistent, data itself is corrupted, etc. Often, issues in data format affect multiple engineers in the same team (e.g., speech recognition team) as they often share the same training data or reference model.

4.2.3 Runtime to Failure

Column 4 of Table 7 presents runtime to failure (RTF) for each classified failure reason. To capture the summary of RTF

distribution, in addition to the average, we also present the 50th-percentile (or median) and higher percentiles such as 90th-percentile and 95th-percentile.

The runtime to failure (RTF) exhibits high variability, with mainly short RTFs. Many failures of training jobs happen quickly, for example within 10 mins. This is mostly the case for failures driven by users in syntax, semantic, and configuration errors, which we can also infer from low median RTFs in the corresponding failure reasons. Note that most of those failures are deterministic and are caught when the runtime begins to execute the program. One of exceptions that is noteworthy is failure corresponding to inconsistent/corrupted input data. We can only detect this at the moment we actually read the erroneous data and attempt to parse it. This is the primary reason for having high 95th-percentile in *incorrect inputs*.

Infrastructure failures occur infrequently but have much longer runtime to failure (RTF). This analysis focuses on two failure reasons in infrastructure category: *model checkpoint error* and *MPI runtime failure*. They represent program-to-storage and program-to-program communication, which are both critical for reliable distributed deep learning training. In general, these errors are relatively infrequent compared to other common errors, constituting only 6.2% of the total Trials. However, our analysis shows that these errors tend to appear after a long execution duration, and thus dominate the time until failure detection. In particular, Table 7 shows that when the corresponding RTFs are summed up (i.e. Total), the two failure reasons, *model checkpoint error* and *MPI runtime error*, occupy as much as 21.73% and 14.63%, respectively.

4.2.4 Impact of GPUs Allocated

For jobs with the same RTF, the impact on the amount of utilized resources is proportional to the number of allocated GPUs. The larger the allocation, the bigger the impact.

Large jobs with programming semantic errors tend to fail a while after execution. Column 5 of Table 7 presents GPU demand across failure reasons. To simplify the analysis, we select four most-dominant failure reasons each contributing around 10% or more in total RTF. When we correlate RTF with GPU demand in Figure 10, among the four failure types, *semantic error* exhibits a markedly distinct trend, with jobs that have higher GPU demand having relatively large RTFs, as compared to jobs having lower GPU demand. This results in disproportional impact on the actual resources utilized by failed jobs. We show this in Column 6 of Table 7.

Column 6 presents actual GPU times for failures while multiplying RTF by GPU demand. As the results show, compared to the RTF only, the impact of *semantic error* increases up to 17.06% from 9.22% while the other three types of failure are either decreased or unchanged. This corresponds to the fact that semantic error is relatively frequent in larger-demand larger-RTF jobs. Looking deeper, we observe that training program instances sometimes send, receive, and access data in an inconsistent way during model parameters synchronization. As a consequence, *semantic error* ranks the second in terms of GPU resources used among failures in our workload.

5 Design Implications for Future Schedulers

Based on our experiences and data-driven analysis so far, in this section we discuss guidelines pertaining to the design of next-generation schedulers for DNN training workloads.

Prioritizing locality. One of the main results from our analysis of GPU scheduling was that lack of locality impacts both utilization and job running time. Our current scheduler adopts a classic approach where it waits for a limited time to see if locality can be achieved and if not the job is scheduled with the resources available at relaxed locality. The main reason for this approach is to keep queuing time low as longer wait times affect user experience.

However given that deep learning jobs run for many hours or even days, incurring a 10% or 20% drop in efficiency could extend the job running time by multiple hours. Thus in such scenarios, waiting for locality for a longer time could be more beneficial. However this requires inferring long-running jobs and appropriately setting user expectations. An alternate strategy could be to *migrate* a job to machines with better locality if resources become available during the execution.

Mitigating interference. Another critical guideline for schedulers would be to consider job placement policies to mitigate inter-job interference. Instead of packing *different* small jobs on a single server, one option would be to place

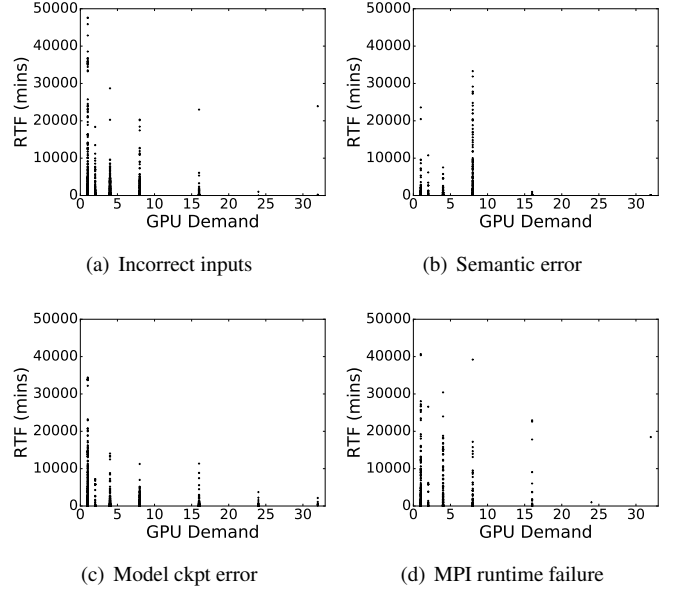


Figure 10: Correlating RTF with GPU demand (i.e., number of GPUs) for four most RTF-dominant failure types.

them on dedicated servers, reducing sharing and thus interference among such jobs. Such an option would increase fragmentation and will result in larger jobs having to wait for longer if we have to prioritize for intra-job locality. Support for job migration to *defragment* the cluster [52], especially applied to smaller jobs, will mitigate interference for small jobs, and will improve intra-job locality for large jobs.

Improving failure handling. A large number of job failures we see come from user errors in code or configuration. This is primarily because programming languages in use are typically not strongly typed. We have found that simple syntax checking could prevent many errors (e.g., missing quotes or parenthesis) and some of the more sophisticated runtime failures can be captured by running the first iteration of training. We plan to set up a pool of cheaper VMs to pre-run jobs. Even running multi-GPU jobs on a single GPU will catch such errors before they run on larger shared clusters and thus prevent *wasted* GPU cycles on them. Training failures also happen due to erroneous data format (e.g., inconsistent columns in samples). We plan to investigate having a well defined schema for datasets used in machine learning, and perform a schema check while accessing data to reduce such errors.

Another useful extension for multi-tenant GPU clusters would be to develop a system to predictively mitigate failures by proactively observing related failures. The main goal of such a system would be to (i) classify error messages in real time from logs that training jobs generate, and (ii) adapting scheduling parameters per job (e.g., number of retries) as well as across jobs (e.g., input data blacklisting) to reduce failure occurrences. For example, the scheduler could stop retrying for failure categories like incorrect inputs and continue retrying for network timeouts.

6 Related Work

Failure analysis of data analytics jobs in shared clusters.

Prior work has looked at designing large-scale data analytics platforms assuming that failures are common [10, 17, 50]. They focus on framework support for fault-tolerance and reliable job execution. In this paper, we focus instead on understanding job failures in deep learning specific platforms.

Kavulya *et al.* conducted a detailed characterization for job failures in a production MapReduce cluster [29]. Some of their findings include: (1) Many jobs fail within a few minutes while the worst-case job takes up to 4.3 days for its failure to be detected. These failures occur due to data copy errors and are similar to HDFS-related failures that we observe taking much longer to detect; (2) Many failures are related to either exceptions due to array indexing errors or IO exceptions. We again see some similarity to our work where coding errors lead to a number of failure cases.

Scheduler and runtime for efficient machine learning execution.

SLAQ schedules concurrent machine learning training jobs based on quality improvement for resource usage, allocating cluster resources for average quality improvement [56]. While this may improve the quality across jobs, each individual job may take longer time to finish. Optimus [37] leverages the convergence curve to predict job remaining time for dynamic resource scheduling and reduces average job completion time. It adopts an online fitting model to derive a proper number of servers and workers for MxNet [15] jobs in parameter server architecture. Tiresias [21] reduces job completion times when many training jobs undergo a *trial-and-error* exploration where job remaining time to complete training cannot be estimated from the convergence curve. In this work, we found that a large job experiences highly varying efficiency over placement spectrum (e.g., Table 5), and that future schedulers may need to consider the trade-off between reducing queueing time and reducing job running time more carefully over a wide range of locality choices.

We also note that an earlier technical report of our work [26] was used to motivate new scheduling primitives in recent work on scheduling like Gandiva [52]. More importantly, our paper presents a systematic study of a large-scale production cluster, covering the whole lifecycle of deep learning jobs including queuing, execution, and failure. We hope that our study of large clusters dedicated to deep learning workloads will continue to motivate novel research in deep learning platforms and schedulers for these workloads.

GPU resource management for machine learning. There are recent efforts on GPU sharing for simpler machine learning tasks. Baymax [14] explores GPU sharing as a way to mitigate both queuing delay and PCIe contention. Following that, Prophet [13] proposes an analytical model to predict performance of GPU workloads. Gandiva [52] proposes GPU time-sharing in shared GPU clusters through checkpointing at

low GPU memory usage of training job. Future work includes integrating these prior work to improve cluster utilization and capacity to run more jobs.

Many training networks are memory bound, especially by capacity. Ryu *et al.* analyzed memory allocation for ImageNet [24], with recent VGG-16 model consuming up to 28 GB of memory [40]. Therefore, vDNN [40] proposes virtualized memory manager, and SuperNeurons [51] adopts fine-grained layer-wise memory control to schedule memory flexibly between CPU and GPU. Our work shares some similarity with prior findings (*i.e.*, some large networks do not fit in GPU memory) in real-world data.

Approximate data processing. Approximate data processing allows trading off accuracy for earlier completion times [6, 9, 16, 23, 27, 55]. In databases, online aggregation has been studied in the context of SQL queries [16, 23, 55]. More recently, approximation has been used in batch processing [6, 8, 49]. Machine learning training presents a fertile ground for exploring trading off accuracy for early completion. In this paper, for the training workloads run on our clusters, we quantify how trading off a very small amount of accuracy (0.1%) can result in significant savings in GPU execution time.

7 Conclusion

In this paper we analyzed a trace of deep learning jobs run on a large multi-tenant cluster of GPUs and studied various factors that affect cluster utilization. Our findings indicated the importance of locality for distributed training jobs and also how interference from other colocated jobs could lead to lower GPU utilization. We also performed a detailed analysis of various failure causes and showed how errors from various parts of the stack contribute to failures. Based on our data analysis and experiences running a large-scale operation, we also described guidelines that could help future research and development of machine learning schedulers.

Finally, we have publicly released the scheduler trace containing information about job arrivals, job size, placement and runtime to the community (details available at [38]). As far as we know, this is the only trace that includes rich information about deep learning training jobs run in production. By making such a trace available, we hope to spur future research in this area.

Acknowledgments

We thank our shepherd, David Nellans, and the anonymous reviewers for their valuable comments and suggestions. We also thank Lidong Zhou, Chris Basoglu, Daniel Li, Marko Radmilac, Ashish Raniwala, Swapnil Palod and the rest of the Microsoft Philly team for their unwavering help

and support. This work was supported in part by NRF-2018R1C1B5086586.

References

- [1] Deep Learning for Siri's Voice. <https://machinelearning.apple.com/2017/08/06/siri-voices.html>.
- [2] Hadoop: Fair Scheduler. <https://hadoop.apache.org/docs/r2.7.2/hadoop-yarn/hadoop-yarn-site/FairScheduler.html>.
- [3] NVIDIA Management Library. <https://developer.nvidia.com/nvidia-management-library-nvml>.
- [4] Using Deep Learning to Create Professional-Level Photographs. <https://research.googleblog.com/2017/07/using-deep-learning-to-create.html>.
- [5] Martín Abadi, Paul Barham, Jianmin Chen, Zhifeng Chen, Andy Davis, Jeffrey Dean, Matthieu Devin, Sanjay Ghemawat, Geoffrey Irving, Michael Isard, et al. TensorFlow: A System for Large-Scale Machine Learning. In *OSDI*, 2016.
- [6] Sameer Agarwal, Barzan Mozafari, Aurojit Panda, Henry Milner, Samuel Madden, and Ion Stoica. BlinkDB: Queries with Bounded Errors and Bounded Response Times on Very Large Data. In *EuroSys*, 2013.
- [7] Ganesh Ananthanarayanan, Sameer Agarwal, Srikanth Kandula, Albert Greenberg, Ion Stoica, Duke Harlan, and Ed Harris. Scarlett: Coping with Skewed Content Popularity in Mapreduce Clusters. In *EuroSys*, 2011.
- [8] Ganesh Ananthanarayanan, Michael Chien-Chun Hung, Xiaoqi Ren, Ion Stoica, Adam Wierman, and Minlan Yu. GRASS: Trimming Stragglers in Approximation Analytics. In *NSDI*, 2014.
- [9] Brian Babcock, Surajit Chaudhuri, and Gautam Das. Dynamic Sample Selection for Approximate Query Processing. In *SIGMOD*, 2003.
- [10] Luiz André Barroso, Jeffrey Dean, and Urs Hölzle. Web Search for a Planet: The Google Cluster Architecture. *IEEE Micro*, 23(2):22–28, March 2003.
- [11] Eric Boutin, Jaliya Ekanayake, Wei Lin, Bing Shi, Jingren Zhou, Zhengping Qian, Ming Wu, and Lidong Zhou. Apollo: Scalable and Coordinated Scheduling for Cloud-scale Computing. In *OSDI*, 2014.
- [12] Ronnie Chaiken, Bob Jenkins, Per-Åke Larson, Bill Ramsey, Darren Shakib, Simon Weaver, and Jingren Zhou. SCOPE: Easy and Efficient Parallel Processing of Massive Data Sets. *VLDB*, 2008.
- [13] Quan Chen, Hailong Yang, Minyi Guo, Ram Srivatsa Kannan, Jason Mars, and Lingjia Tang. Prophet: Precise QoS Prediction on Non-Preemptive Accelerators to Improve Utilization in Warehouse-Scale Computers. In *ASPLOS*, 2017.
- [14] Quan Chen, Hailong Yang, Jason Mars, and Lingjia Tang. Baymax: QoS Awareness and Increased Utilization for Non-Preemptive Accelerators in Warehouse Scale Computers. In *ASPLOS*, 2016.
- [15] Tianqi Chen, Mu Li, Yutian Li, Min Lin, Naiyan Wang, Minjie Wang, Tianjun Xiao, Bing Xu, Chiyuan Zhang, and Zheng Zhang. MXNet: A Flexible and Efficient Machine Learning Library for Heterogeneous Distributed Systems. *arXiv preprint arXiv:1512.01274*, 2015.
- [16] Tyson Condie, Neil Conway, Peter Alvaro, Joseph M. Hellerstein, John Gerth, Justin Talbot, Khaled Elmeleegy, and Russell Sears. Online Aggregation and Continuous Query Support in MapReduce. In *SIGMOD*, 2010.
- [17] Jeffrey Dean and Luiz André Barroso. The Tail at Scale. *Commun. ACM*, 56(2):74–80, February 2013.
- [18] Dror G Feitelson. Packing schemes for gang scheduling. In *Workshop on Job Scheduling Strategies for Parallel Processing*, pages 89–110. Springer, 1996.
- [19] Ian Goodfellow, Yoshua Bengio, Aaron Courville, and Yoshua Bengio. *Deep Learning*, volume 1. MIT press Cambridge, 2016.
- [20] Priya Goyal, Piotr Dollár, Ross Girshick, Pieter Noordhuis, Lukasz Wesolowski, Aapo Kyrola, Andrew Tulloch, Yangqing Jia, and Kaiming He. Accurate, Large Minibatch SGD: Training ImageNet in 1 Hour. *arXiv preprint arXiv:1706.02677*, 2017.
- [21] Juncheng Gu, Kang G. Chowdhury, Mosharaf abd Shin, Yibo Zhu, Myeongjae Jeon, Junjie Qian, Hongqiang Liu, and Chuanxiong Guo. Tiresias: A GPU Cluster Manager for Distributed Deep Learning. In *NSDI*, 2019.
- [22] Kaiming He, Xiangyu Zhang, Shaoqing Ren, and Jian Sun. Deep Residual Learning for Image Recognition. In *CVPR*, 2016.
- [23] Joseph M. Hellerstein, Peter J. Haas, and Helen J. Wang. Online Aggregation. In *SIGMOD*, 1997.
- [24] ImageNet, 2016. <http://image-net.org>.
- [25] Michael Isard, Vijayan Prabhakaran, Jon Currey, Udi Wieder, Kunal Talwar, and Andrew Goldberg. Quincy: Fair Scheduling for Distributed Computing Clusters. In *SOSP*, 2009.
- [26] Myeongjae Jeon, Shivaram Venkataraman, Amar Phanishayee, Junjie Qian, Wencong Xiao, and Fan Yang. Multi-tenant GPU Clusters for Deep Learning Workloads: Analysis and Implications. Technical Report MSR-TR-2018-13, 2018.
- [27] Chris Jermaine, Subramanian Arumugam, Abhijit Pol, and Alin Dobra. Scalable Approximate Query Processing with the DBO Engine. *ACM Trans. Database Syst.*, 33(4):23:1–23:54, December 2008.
- [28] Yangqing Jia, Evan Shelhamer, Jeff Donahue, Sergey Karayev, Jonathan Long, Ross Girshick, Sergio Guadarrama, and Trevor Darrell. Caffe: Convolutional Architecture for Fast Feature Embedding. In *MM*, 2014.
- [29] Soila Kavulya, Jiaqi Tan, Rajeev Gandhi, and Priya Narasimhan. An Analysis of Traces from a Production MapReduce Cluster. In *CCGRID '10*, 2010.
- [30] Alex Krizhevsky, Ilya Sutskever, and Geoffrey E Hinton. ImageNet Classification with Deep Convolutional Neural Networks. In *NIPS*, 2012.
- [31] Mu Li, David G Andersen, Jun Woo Park, Alexander J Smola, Amr Ahmed, Vanja Josifovski, James Long, Eugene J Shekita, and Bor-Yiing Su. Scaling Distributed Machine Learning with the Parameter Server. In *OSDI*, 2014.
- [32] Matthew L Massie, Brent N Chun, and David E Culler. The Ganglia Distributed Monitoring System: Design, Implementation And Experience. *Parallel Computing*, 30(7):817–840, 2004.
- [33] Avner May, Alireza Bagheri Garakani, Zhiyun Lu, Dong Guo, Kuan Liu, Aurélien Bellet, Linxi Fan, Michael Collins, Daniel Hsu, Brian Kingsbury, et al. Kernel Approximation Methods for Speech Recognition. *arXiv preprint arXiv:1701.03577*, 2017.
- [34] Tomáš Mikolov, Martin Karafiát, Lukáš Burget, Jan Černocký, and Sanjeev Khudanpur. Recurrent Neural Network Based Language Model. In *Eleventh Annual Conference of the International Speech Communication Association*, 2010.
- [35] Open Platform for AI, 2018. <https://github.com/microsoft/pai>.
- [36] Kay Ousterhout, Patrick Wendell, Matei Zaharia, and Ion Stoica. Sparrow: Distributed, Low Latency Scheduling. In *SOSP*, 2013.
- [37] Yanghua Peng, Yixin Bao, Yangrui Chen, Chuan Wu, and Chuanxiong Guo. Optimus: An Efficient Dynamic Resource Scheduler for Deep Learning Clusters. In *EuroSys*, 2018.
- [38] DNN training workloads on Microsoft's internal Philly clusters, 2019. <https://github.com/msr-fiddle/philly-traces>.
- [39] PyTorch, 2018. <https://pytorch.org/>.
- [40] Minsoo Rhu, Natalia Gimelshein, Jason Clemons, Arslan Zulfiqar, and Stephen W Keckler. vDNN: Virtualized Deep Neural Networks for Scalable, Memory-efficient Neural Network Design. In *MICRO*, 2016.

- [41] Malte Schwarzkopf, Andy Konwinski, Michael Abd-El-Malek, and John Wilkes. Omega: Flexible, Scalable Schedulers for Large Compute Clusters. In *EuroSys*, 2013.
- [42] Frank Seide and Amit Agarwal. CNTK: Microsoft’s Open-Source Deep-Learning Toolkit. In *KDD*, 2016.
- [43] Konstantin Shvachko, Hairong Kuang, Sanjay Radia, and Robert Chansler. The Hadoop Distributed File System. In *MSST*, 2010.
- [44] Apache Hadoop 3.2.0 Submarine, 2019. <https://hadoop.apache.org/docs/r3.2.0/hadoop-yarn/hadoop-yarn-applications/hadoop-yarn-submarine/>.
- [45] Martin Sundermeyer, Ralf Schlüter, and Hermann Ney. LSTM Neural Networks for Language Modeling. In *Thirteenth Annual Conference of the International Speech Communication Association*, 2012.
- [46] Christian Szegedy, Wei Liu, Yangqing Jia, Pierre Sermanet, Scott Reed, Dragomir Anguelov, Dumitru Erhan, Vincent Vanhoucke, and Andrew Rabinovich. Going Deeper With Convolutions. In *CVPR*, 2015.
- [47] Ashish Vaswani, Noam Shazeer, Niki Parmar, Jakob Uszkoreit, Llion Jones, Aidan N Gomez, Łukasz Kaiser, and Illia Polosukhin. Attention Is All You Need. In *NIPS*, 2017.
- [48] Vinod Kumar Vavilapalli, Arun C Murthy, Chris Douglas, Sharad Agarwal, Mahadev Konar, Robert Evans, Thomas Graves, Jason Lowe, Hitesh Shah, Siddharth Seth, et al. Apache Hadoop YARN: Yet Another Resource Negotiator. In *SoCC*, 2013.
- [49] Shivaram Venkataraman, Aurojit Panda, Ganesh Ananthanarayanan, Michael J. Franklin, and Ion Stoica. The Power of Choice in Data-aware Cluster Scheduling. In *OSDI*, 2014.
- [50] Abhishek Verma, Luis Pedrosa, Madhukar Korupolu, David Oppenheimer, Eric Tune, and John Wilkes. Large-scale Cluster Management at Google with Borg. In *EuroSys*, 2015.
- [51] Linnan Wang, Jinmian Ye, Yiyang Zhao, Wei Wu, Ang Li, Shuaiwen Leon Song, Zenglin Xu, and Tim Kraska. Superneurons: Dynamic GPU Memory Management for Training Deep Neural Networks. In *PPoPP*, 2018.
- [52] Wencong Xiao, Romil Bhardwaj, Ramachandran Ramjee, Muthian Sivathanu, Nipun Kwatra, Zhenhua Han, Pratyush Patel, Xuan Peng, Hanyu Zhao, Quanlu Zhang, Fan Yang, Lidong Zhou. Gandiva: Introspective Cluster Scheduling for Deep Learning. In *OSDI*, 2018.
- [53] Hangchen Yu and Christopher J. Rossbach. Full Virtualization for GPUs Reconsidered. In *Workshop on Duplicating, Deconstructing, and Debunking (WDDD)*, 2017.
- [54] Matei Zaharia, Dhruba Borthakur, Joydeep Sen Sarma, Khaled Elmelegy, Scott Shenker, and Ion Stoica. Delay Scheduling: A Simple Technique for Achieving Locality and Fairness in Cluster Scheduling. In *EuroSys*, 2010.
- [55] Kai Zeng, Sameer Agarwal, and Ion Stoica. iOLAP: Managing Uncertainty for Efficient Incremental OLAP. In *SIGMOD*, 2016.
- [56] Haoyu Zhang, Logan Stafman, Andrew Or, and Michael J. Freedman. SLAQ: Quality-driven Scheduling for Distributed Machine Learning. In *SoCC*, 2017.